COBEM-2019-1130
ASSESSMENT OF ELECTRIFICATION ON CONCEPTUAL DESIGN OF A THIN HAUL AIRCRAFT

Higor Luis Silva
Thiago Augusto Machado Guimarães
Federal University of Uberlândia, School of Mechanical Engineering, Uberlândia, MG, 38400-902, Brazil
higor@ufu.br, thiagoamg@ufu.br

Abstract. *In recent years, the scientific community and several governmental organizations around the world have been discussing ways to reduce pollutant emissions and other environmental issues. Moreover, the means of transport are included in these debates, making the aerospace industry to develop new technologies and aircraft more efficient and "green". Thus, electric and hybrid-electric propulsion systems are designed in aviation to contribute to the reduction of pollutant emissions, but, as a consequence, they bring new design concepts and performance gains, such as reduction of fuel consumption. In this context, this paper presents the effects that powertrain with distributed propulsion produces on the conceptual design of an aircraft, i.e., what are the improvements brought by such a system. By means of parametric analyses, the influences of some fundamental parameters, such as number of engines and fraction of wingspan occupied by the DP array, are shown. The results showed that electrification brings great benefits in conceptual design, increasing the feasible design space, which allows smaller wings and smaller powertrains. In addition, there is an improvement in performance, enabling applications in flight operations such as thin haul aircraft, which are used as an example of application.*

Keywords: aircraft design, hybrid-electric aircraft, thin haul aircraft, distributed propulsion.

1. INTRODUCTION

Over the past decade, many institutions, such as NASA (Bonet *et al.*, 2011) and the European Commission (ACARE, 2012), have set many targets for reducing carbon emissions and other pollutants for the next years. The aerospace industry is directly affected by these new requirements, since it is one of the main contributors in the emission of pollutants. Moreover, seeking a more efficient development that meets this demand, NASA has set performance targets for the next generations of aircraft, which include, for the next 20 years, a reduction of -55 dB at the airport boundary, -75% NOx, and -70% fuel burn relative to the reference year of 2006 (NASA, 2012).

Furthermore, to achieve such results, engineers have invested research into the development of disruptive technologies that are capable of generating more efficient and "greener" aircraft. Many unconventional aircraft projects have come up to meet such expectations, along with electric and hybrid-electric propulsion systems. These systems are defined in terms of design requirements and aircraft type, but the installation of energy storage systems, such as batteries, are generally used to reduce fuel consumption. Other concepts and systems, such as Boundary Layer Ingestion (BLI) and Distributed Propulsion (DP), have recently been studied in order to improve aircraft aerodynamics, which benefits the entire project (Felder *et al.*, 2009). DP, for example, comprises a set of electric propulsors usually installed along the wing, which generates air-propulsive interactions that result in gains in propulsion and total-lift of the aircraft (Gohardani *et al.*, 2011).

Along those lines, due to the improvements brought by those new concepts, some aviation markets may finally become profitable, as is the case of thin haul transportation. This operation refers to the air transportation of passengers on very small capacity aircraft over ultra-short distances (Justin *et al.*, 2017); in other words, it is not very attractive for airlines to operate. As presented by Harish *et al.* (2016), to achieve economic viability, the thin haul transportation must increase the revenue potential through innovative pricing and scheduling, while drastically reducing operating costs, in particular, energy, maintenance, and labor costs. Then, some research has been devoted to study new proposals. Stoll and Veble Mikic (2016), for example, present a conceptual design study of a distributed electric propulsion transport aircraft. Hwang and Ning (2018) proposes a large-scale multidisciplinary optimization of an electric aircraft for on-demand mobility. Justin *et al.* (2017) focus on the estimation of the operating cost reduction and in particular the reduction in energy expenditures when transitioning from a current commuter aircraft to an advanced state-of-the-art electric aircraft featuring several game-changing technologies

This paper proposes an assessment of electrification on conceptual design of a thin haul aircraft. The hybrid-electric architectures associated to propulsive systems and the effects of distributed propulsion in the conceptual design of hybrid-

electric aircraft is presented. Constraint diagrams are used to define the feasible design spaces and to help in choosing the optimum design points, favoring specific components. Parametric analyzes are performed to evaluate the influence of some parameters, such as number of propulsors and fraction of wingspan occupied by the DP array. The thin haul aircraft is chosen as an example of application due to its current appeal, which shows that the electrification of propulsive systems enables non-profit operations.

2. CONSTRAINT DIAGRAMS

The constraint diagram is a well-known method (Torenbeek, 2013) used to represent the different performance constraints of an aircraft and the resulting feasible design space in terms of wing loading and thrust-to-weight ratio (or power loading). Then, from this feasible design space, it is possible to define the wing area and the installed power, which are, initially, the main step when designing an aircraft. Currently, the studies performed around the world have been considering different configurations for the powertrain, such as Distributed Propulsion (DP), which is the spreading of propulsive elements (i.e., fans, propellers, or jets) over the airframe in a beneficial manner (Gohardani *et al.*, 2011), as illustrated in Fig. 1. This approach has estimated improvements propulsive efficiency through, for example, reduced wing area (Borer *et al.*, 2016) or increased effective bypass ratio (Felder *et al.*, 2009). Thus, it is discussed here hybrid systems that present synergistic benefits when combined with distributed propulsion, being referred to as *hybrid-electric distributed propulsion* (HEDP).
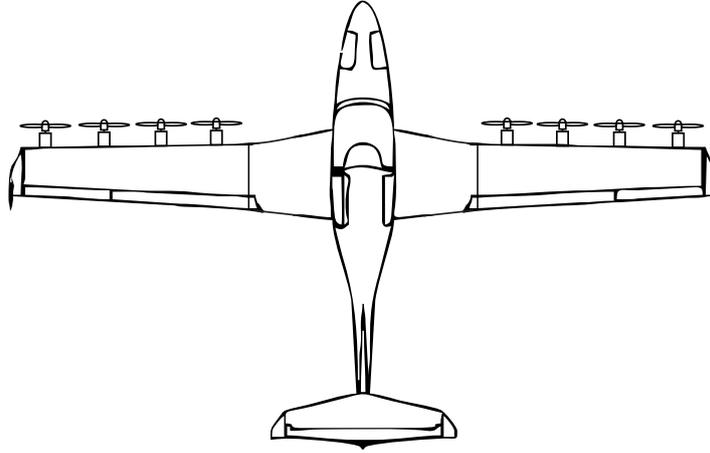

Figure 1. Schematic representation of distributed propulsion along the wing.

In conventional aircraft designs, propulsive effects are not taken into account in aerodynamic calculations (lift and drag). In other words, the sizing methods are simplified. However, when having configurations with distributed propulsion, it is important to take into account these effects, since they directly modify the aerodynamic flow throughout the aircraft, which results in different lift and drag components. Nonetheless, the DP contributes directly to the thrust, i.e., the total thrust of the aircraft (T) is the sum of the component produced by the conventional propulsors (T_0), and the component produced by the array of distributed propulsors installed over the wing (T_{dp}), which presents strong interaction effects with the airframe. Thus,

$$T = T_0 + T_{dp} \tag{1}$$

and the total lift produced by the aircraft can be expressed as

$$L = L_{\text{airframe}} + \Delta L(T_{dp}, L_{\text{airframe}}, S, \dots) \tag{2}$$

where ΔL is the increase in aircraft lift due to the thrust generated by the distributed propulsors, which depends on thrust, airframe lift and a fraction of wing area. Nonetheless, the aero-propulsive interaction generates effects on the overall drag of the aircraft, as expressed:

$$D = \underbrace{D_0 + \Delta D_0(T_{dp}, S, \dots)}_{\text{zero-lift drag}} + \underbrace{D_i(L_{\text{airframe}}) + \Delta D_i(T_{dp}, L_{\text{airframe}}, S, \dots)}_{\text{lift-induced drag}} \tag{3}$$

where D_0 is the zero-lift drag without distributed propulsors, ΔD_0 is the increase in zero-lift due to the DP system. This increase can be caused by interaction with jets or slipstreams at zero lift, by variations in angle of attack in order to maintain zero lift, or by changes in wetted area due to pylons, nacelles, and other external elements of the propulsion-system installation. Moreover, D_i is the lift-induced drag of the aircraft without DP, and ΔD_i is the change in lift-induced drag due to the DP system.

Therefore, the aero-propulsive interaction effects of the distributed propulsors are expressed by means of these "Deltas", which are estimated using detailed aerodynamic analyses. For the conceptual sizing phase, surrogate models or simplified aerodynamic models have been proposed recently. This work uses the model proposed by de Vries *et al.* (2018) along with the aerodynamic analysis presented by Patterson *et al.* (2015).

For a general flight, the main forces acting on an aircraft in flight are shown in the free-body diagram in Fig. 2, where W is the weight of the aircraft, V the velocity vector, γ the flight path angle, and μ the bank angle. For conventional aircraft, there is only the thrust component aligned to the velocity vector (T_0); however, here there is an additional component (T_{dp}), which is produced by the DP system.

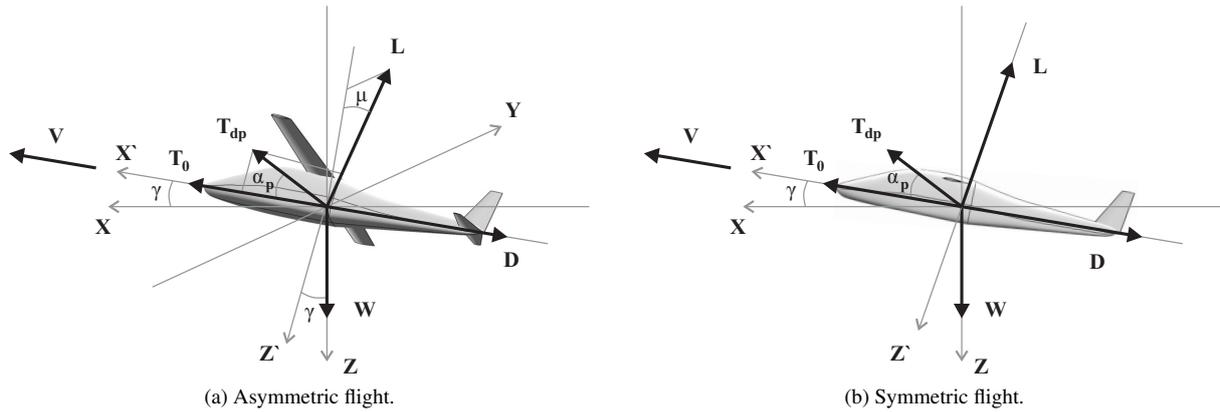(a) Asymmetric flight.　　　　　　　　　　　　　　(b) Symmetric flight.

Figure 2. Schematic representation of the forces acting on the aircraft point model.

Applying Newton's Law and solving the equilibrium equations in order to find a correlation for the thrust-to-weight (T/W) and wing loading (W/S), the following equations are obtained:

$$\frac{T}{W} = \frac{\dfrac{q_\infty}{(W/S)} \left(C_{D_0} + \Delta C_{D_0} + \dfrac{C_{L_{\text{airframe}}}^2}{\pi e \mathcal{R}} + \Delta C_{D_i} \right) + \dfrac{\dot{h}}{V} + \dfrac{1}{g}\dfrac{dV}{dt}}{1 - \chi(1 - \cos\alpha_p)} \tag{4}$$

$$\frac{W}{S} = \frac{q_\infty \cos\mu \left(C_{L_{\text{airframe}}} + \Delta C_L \right)}{\sqrt{1 - \left(\dfrac{\dot{h}}{V} \right)^2} - \chi \sin\alpha_p \cos\mu \left(\dfrac{T}{W} \right)} \tag{5}$$

where q_∞ is the dynamic pressure, C_D the drag coefficient, C_L the lift coefficient, e the Oswald factor, $\mathcal{R}$ the aspect ratio, $\dot{h}$ the rate of climb, V the airspeed, α_p the angle between the propulsors and the airspeed vector, μ the bank angle, χ the percentage of the total propulsion force that is due to the distributed propulsive system, and the "Deltas" represent the aero-propulsive effects due to the DP.

The Equations (4) and (5) are intrinsic equations, so they have to be solved iteratively and assuming some conditions, which depend on each flight phase. For cruise phase, the airspeed is constant and the lift coefficient varies. In the climb phase, the lift coefficient is constant and the airspeed varies. For takeoff is used the formulation presented by Raymer (2012), and the approach condition is estimated using $1.2V_{\text{approach}}$.

Usually, the two axes represent parameters such as (y-axis) thrust-to-weight ratio (T/W) and (x-axis) wing loading (W/S). However, for HEDP aircraft, the use of power-loading (W/P) on the y-axis is better for some reasons. First, there are propellers installed, so power loading is more suitable for the case. Secondly, the power produced by the propulsive elements is required to size the components of the powertrain, and not thrust. Finally, when selecting the optimum design, it is convenient to select the powertrain that has to produce the least amount of power (which is directly related to energy consumption), not thrust.

Traditionally, among all the T/W and W/S combinations that allow meeting the mission performance, the designer should choose the design point that yield the aircraft with the lowest cost and weight. Therefore, the optimal design point is chosen for:

1. the *highest possible wing loading*, i.e., smallest wing, and

2. the *lowest possible thrust-to-weight ratio* or *highest possible power loading*, i.e., smallest engine.

To switch a thrust-to-weight ratio (T/W) curve into a power loading (W/P) curve, the following relation can be used:

$$\frac{W}{P} = \frac{1}{V(T/W)} \tag{6}$$

Lastly, the curves can be plotted on a constraint diagram and, finally, obtaining the *feasible design space*, a region under the curves where all performance constraints are satisfied for any of the W/P and W/S combinations.

As already discussed, for fuel-based aircraft, the goal is to identify the combination of maximum wing loading and minimum thrust loading (maximum power loading for propeller aircraft) that allow meeting all the given performance requirements, for certain assumptions on $\mathcal{R}$ and $C_{L_{\max}}$. Here, for HEDP aircraft, picking a design point depends on the figure of merit that the designer wants to minimize.

3. THIN HAUL AIRCRAFT

Thin haul transportation refers to the air transportation of passengers on very small capacity aircraft over ultra-short distances (Justin *et al.*, 2017). This type of operation has received attention in the last debates on aircraft electrification, as these hybrid and electric aircraft can make this type of transport feasible again.

Air transportation from small and medium airports is severely restricted by harsh economic realities. In the deregulated market, carriers choose to provide service only if and when operations are sufficiently profitable (Bhattacharyya *et al.*, 2017). But even with the Essential Air Service (EAS) program, which is a U.S. government program to maintain a minimal level of scheduled air service to communities that are not very profitable, it is not economically feasible for established airlines operating large aircraft to serve the majority of the thousands of airports (and potential routes) in the United States. Many of the routes that can support service by airlines can only do so at very low frequency, diminishing the value to passengers. Many carriers have found a solution in using smaller airports either with higher-frequency scheduled flights with smaller aircraft or by offering an on-demand air taxi service. Despite the higher per-seat-mile cost of operating smaller aircraft, demand has been shown to increase on routes once a reasonable frequency and availability can be achieved.

From this context, for the example of application, it is selected a domestic transport aircraft for thin haul scheduled or on-demand operations servicing small airports and short routes. The proposed aircraft is in the market of the Piper PA-46 and Cirrus SR22, and the general requirements and constraints of the aircraft are summarized in Table 1.

Table 1. Requirements and constraints of the thin haul aircraft.

Parameter	Value
Number of passengers	4-6
Payload, W_{PL} [lbs]	800
Range, R [nmi]	250
Cruise altitude, h_{cr} [ft]	17500
Cruise Mach number, M_{cr} [-]	0.3
Approach speed, V_{app} [KCAS]	110
OEI climb gradient, $\dot{h}/V$ [%]	2.1
OEI climb speed, V_{climb} [knots]	$1.4V_{SR}$
Takeoff field length, S_{TO} [m]	2375

Notwithstanding, two powertrain architectures will be evaluated: a conventional and a serial with a distributed propulsion system, as illustrated in Fig. 3. The respective selected design parameters are shown in Table 2, and the aerodynamic assumptions in Table 3. More details of the formulation, variables and assumptions are available in Silva (2019).
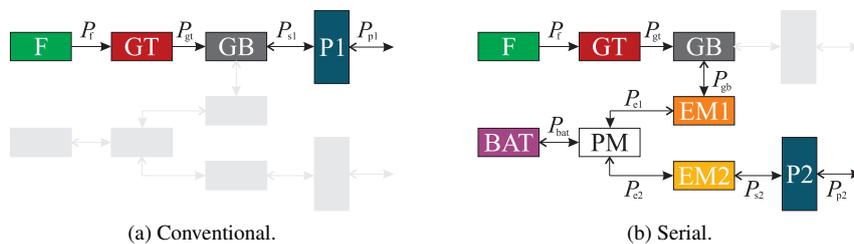

(a) Conventional. (b) Serial.

Figure 3. Powertraing architectures considered. Legend: "F" = fuel, "GT"= gas turbine, "GB"= gearbox, "P"= propulsor, "BAT"= batteries, "EM"= electrical machine (i.e. electric motor or generator), "PM"= power management.

Table 2. Selected design parameters for the thin haul aircraft.

Parameter	Value
Aspect Ratio, $\mathcal{R}$ [-]	10
Half-chord sweep, $\Lambda_{c/2}$ [deg]	0
N^o propulsors*, N [-]	8
DP span fraction*, $\Delta y_{dp}/b$ [-]	0.6
Spacing between DP propulsors*, δ_y [-]	0.01
Axial position of DP propulsors*, x_p/c [-]	-0.2
EM efficiency*, η_{EM1} or η_{EM2} [-]	0.96
PM efficiency*, η_{PM} [-]	0.99
Gearbox efficiency, η_{GB} [-]	0.96
Gas turbine efficiency, η_{GT} [-]	0.3

Table 3. Aerodynamic assumptions for the thin haul aircraft.

Parameter	Cruise	Approach	Takeoff	OEI climb
Flap configuration	clean	landing	takeoff	landing
Landing gear position	retracted	extended	extended	retracted
Zero-lift drag coefficient, C_{D_0}	0.021	0.106	0.055	0.65
Oswald factor, e	0.78	0.88	0.81	0.88
Maximum lift coefficient, $C_{L_{\text{max,airframe}}}$	–	2.5	2.0	2.5
Propulsive efficiency (primary)*, η_{p1}	0.9	0.8	0.75	0.8
Propulsive efficiency (secondary)*, η_{p2}	0.85	0.75	0.7	0.75
Supplied power ratio*, $\Phi = P_{\text{bat}}/(P_{\text{bat}} + P_{\text{f}})$	0.05	0.2	0.1	0.2

4. RESULTS AND DISCUSSION

Solving Equations (4) and (5), it is evaluated the four types of performance constraints, as discussed previously. The four constraint curves for the serial configuration are shown in Fig. 4.

Combining the four constraint curves from Fig. 4, and doing the same process for the conventional configuration, it is possible to plot the total power-loading diagrams for both powertrain architectures, which are shown in Fig. 5. Comparing both diagrams, one can notice that the feasible design space is bigger for the serial architecture. This happens because for the serial configuration there is a distributed propulsion system installed, which produces aero-propulsive interactions, causing an increase of lift. Thus, the feasible design space provides better choices for the optimum design points, as will be discussed next.

Making the breaking down of the power-loading in terms of the components, i.e., in terms of gas turbine, electric motors, and batteries, it is possible to plot the four power-loading diagrams depicted in Fig. 6. Comparing the $W/P_{\text{GT,max,SL}}$ for the conventional architecture (Fig. 6a) with the $W/P_{\text{GT,max,SL}}$ for the serial architecture, one can see that the feasible design space increased for the serial configuration. Nonetheless, when comparing, for example, the cruise speed curve (in blue) for both configurations, the curve shows higher values for the serial architecture. This happens because in the hybrid-electric configuration, there is a battery participating of the cruise phase, which means that less power is required from the gas turbine. Since any change in power is inversely proportional in the ratio W/P, the curve increases. The same behavior can be observed for the other curves, but with different proportions due to the equation involved.

Regarding the approach speed curve, it is worth noting that the line moves forward, increasing considerably the design space, which directly affects the choice of the optimum design point. This happens because the distributed propulsive system installed generates aero-propulsive interactions which produces a "Delta" C_L. Since the approach speed constraint is straightforwardly related to lift coefficient, the increment in C_L results in an improvement of that requirement. Following the same reasoning, the climb and takeoff constraint curves increase due to this aerodynamic gain.

Still in Figs. 6a and 6b, the choice of the optimum design point, as discussed previously, depends on what the designer is looking for. In other words, in this case, if he or she wants a smaller wing, the point marked with a "star" has to be chosen. On the other hand, if he or she wants to design for minimum gas turbine power, the point marked with an upside-down triangle has to be chosen. In addition, it is interesting to see that in Fig. 6a the climb is the one responsible to limit the design of the gas turbine point, while in Fig. 6b the climb curve is far from the feasible design space. Moreover, the "star" point will always be the most up and right point.
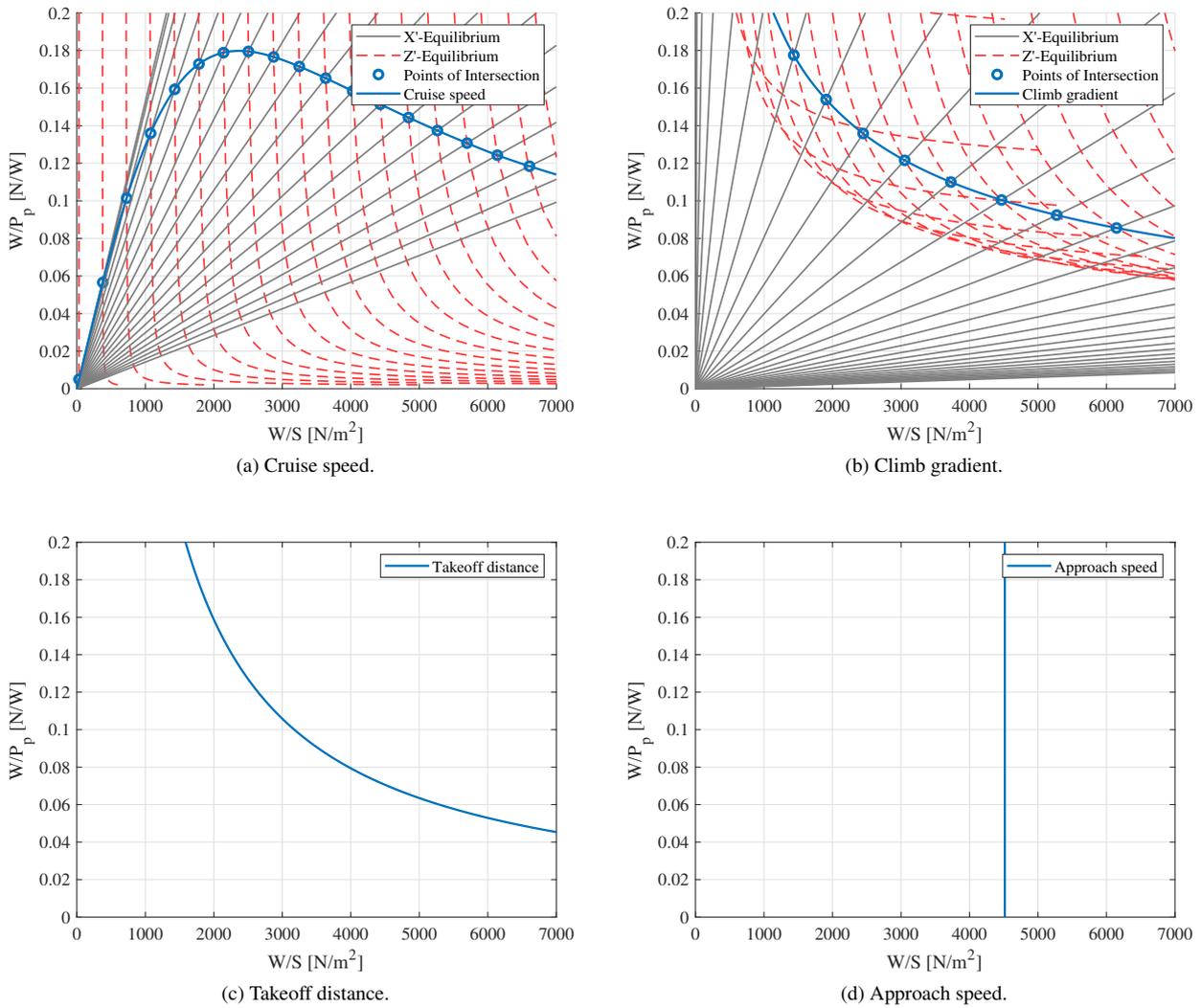
(a) Cruise speed.

(b) Climb gradient.

(c) Takeoff distance.

(d) Approach speed.

Figure 4. Construction of the four constraint curves for the serial configuration.

(a) Conventional.
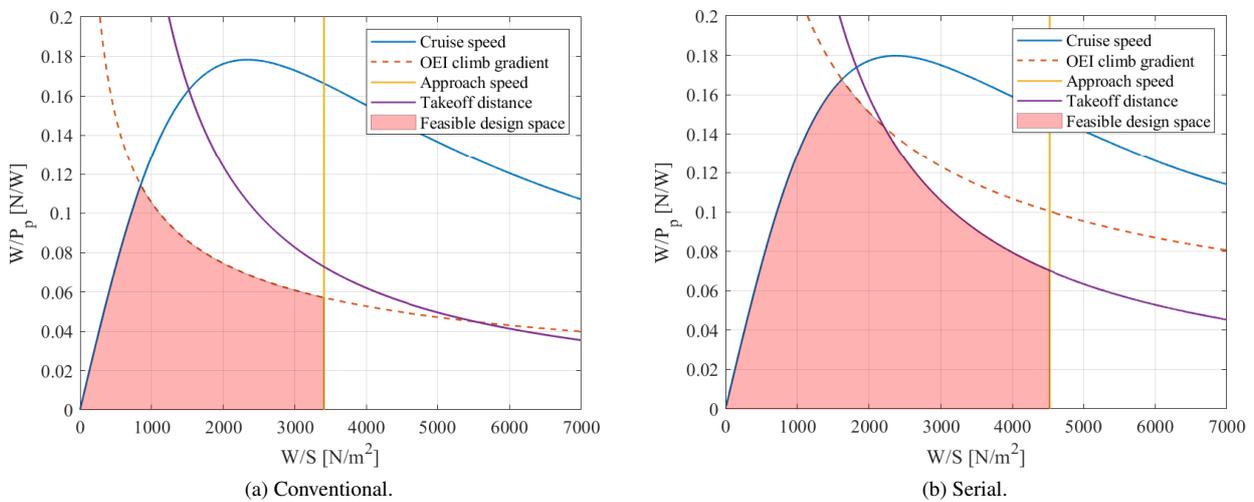
(b) Serial.

Figure 5. Total power loading diagrams for aircraft with conventional and serial powertrain architecture.

(a) $W/P_{\text{GT,max,SL}}$ - Conventional.

(b) $W/P_{\text{GT,max,SL}}$ - Serial.

(c) W/P_{EM2} - Serial.
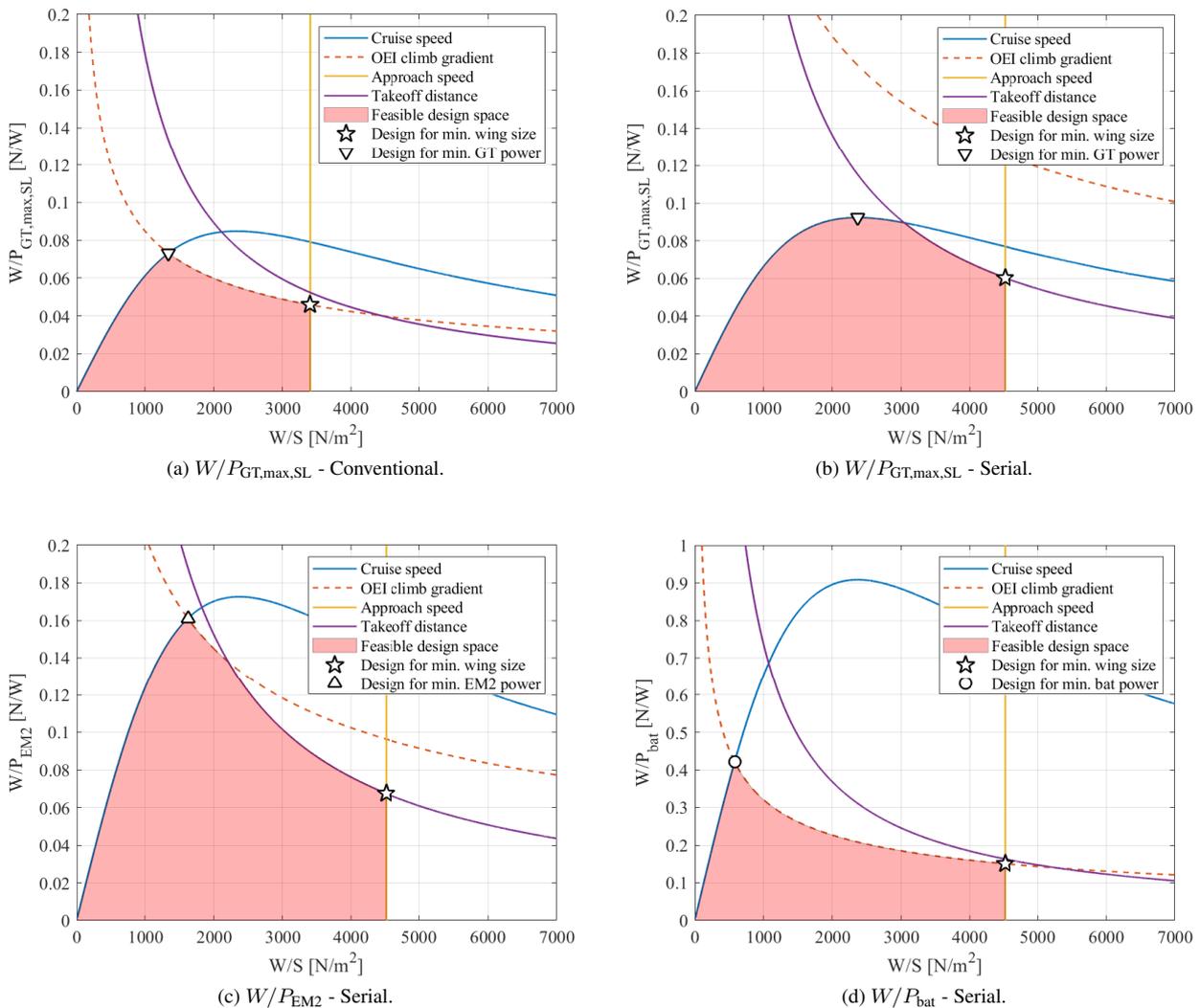
(d) W/P_{bat} - Serial.

Figure 6. Component power loading diagrams for the thin-haul aircraft with conventional and serial architecture.

Moving forward, and repeating the same analysis for the other components, i.e., for the electric motor and battery, two other optimum design points are shown in Figs. 6c and 6d, where the regular triangle represents the choice of design for minimum electric motor power, and the regular circle represents for minimum battery power. Finally, it is important to say that most people would select the design point for maximum wing loading, which usually corresponds to the smallest wing size. However, this is not always the best option. Due to the large impact of the powertrain on MTOW, it may be more beneficial to select one of the other design points, or even a different combination of wing loading and power loading that minimizes MTOW or another figure of merit. This can lead to increased component power-loading, and therefore reduced powertrain weight – assuming that the reduction in powertrain mass is not outweighed by the increase in wing mass.

To evaluate how the distributed propulsion configuration impacts the overall constraint diagram, an additional parametric analysis is performed. The parameters chosen to be changed are the number of propulsors, i.e, electric motors, distributed along the wing (N) and the fraction of wingspan occupied by the DP array ($\Delta y_{dp}/b$).

Varying N from 4 to 8, and $\Delta y_{dp}/b$ from 0.4 and 0.6, the results depicted in Fig. 7 are obtained. As one can see, these parameters affects directly the computation of the "Deltas" of C_L and C_D, which shifts the constraint curves, generating different optimum design points. Even though the correlation of increasing one parameter and the other is not linear, the plots show that when the number of propulsors are increase, for a specific fraction of wingspan occupied by the DP array, the feasible design space increases as well, so it is obtained better optimum design points. This can be verified comparing Figs. from top to bottom in same column. It happens because a more quantity of propulsors distributed along the wing may allow a better aerodynamic flow, which generates better aero-propulsive interactions.
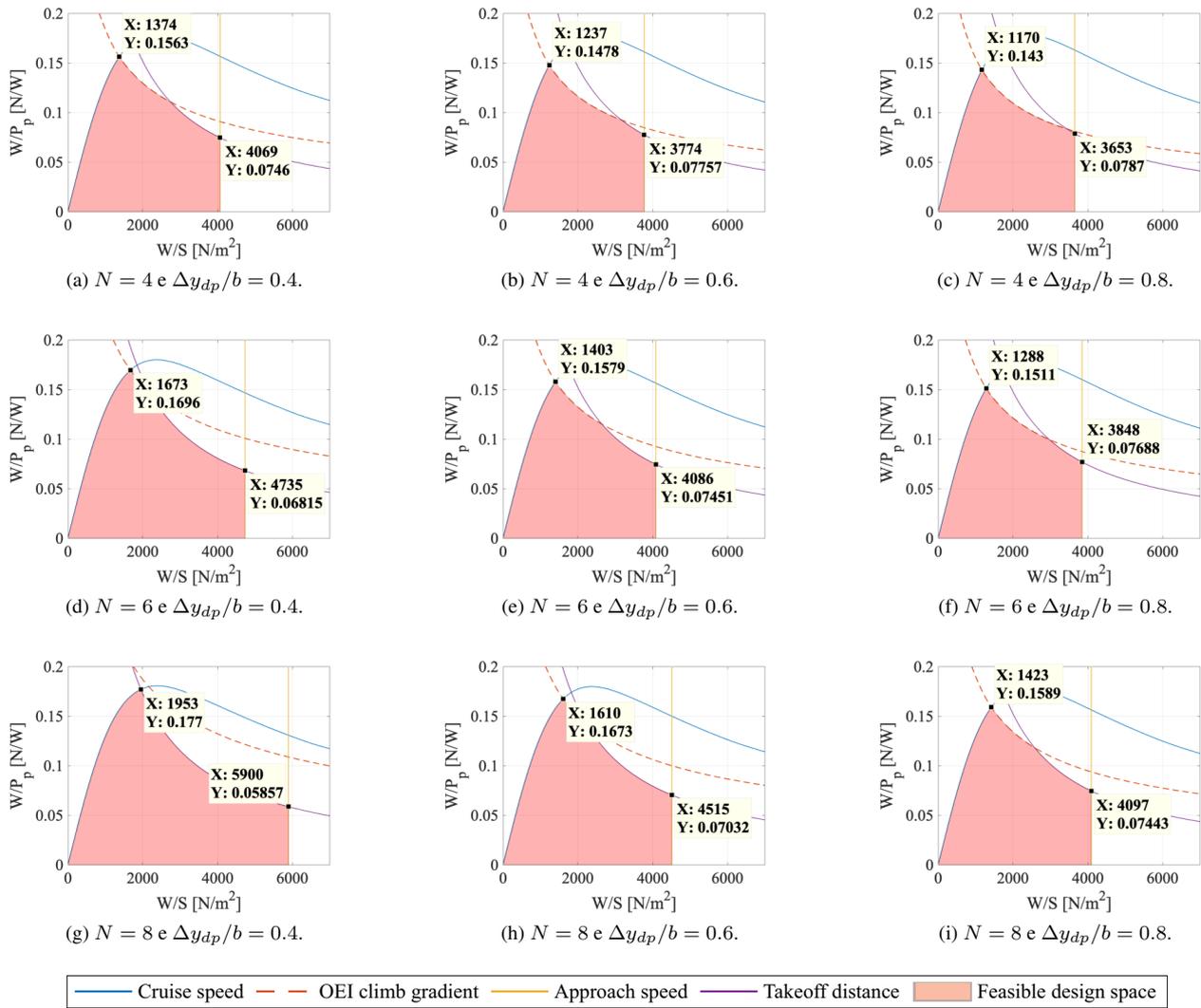
(a) $N = 4$ e $\Delta y_{dp}/b = 0.4$.

(b) $N = 4$ e $\Delta y_{dp}/b = 0.6$.

(c) $N = 4$ e $\Delta y_{dp}/b = 0.8$.

(d) $N = 6$ e $\Delta y_{dp}/b = 0.4$.

(e) $N = 6$ e $\Delta y_{dp}/b = 0.6$.

(f) $N = 6$ e $\Delta y_{dp}/b = 0.8$.

(g) $N = 8$ e $\Delta y_{dp}/b = 0.4$.

(h) $N = 8$ e $\Delta y_{dp}/b = 0.6$.

(i) $N = 8$ e $\Delta y_{dp}/b = 0.8$.

Figure 7. Parametric analysis for the power loading diagrams regarding N e $\Delta y_{dp}/b$.

On the other hand, keeping the number of propulsors constant and increasing the fraction of wingspan occupied by the DP array, the feasible design space decreases, so the optimum design points become worse. This can be verified comparing Figs. from left to right in same line. This happens because for a certain number of propulsors, and keeping the spacing between each one of them constant, their diameter increases, and the aero-propulsive interactions are hampered. The actual causes is not so clear, but it is what the model is able to describe.

5. CONCLUDING REMARKS

This paper presents an assessment of electrification on conceptual design of a thin haul aircraft. The constraint diagrams are able to determine the the feasible design space for a aircraft with distributed propulsive system, being great methods of initial analysis for the conceptual design of an aircraft. The results show that the constraint curves are very sensitive to the parameters assumed (aerodynamic and technological), which makes this stage of the study extremely important. To corroborate this idea, the parametric evaluation exemplified the case where the increase of number of propulsors improves the optimum design points, and the increase of fraction of wingspan occupied by the DP does the opposite. Moreover, it is very clear to see the effects brought by the aero-propulsive interactions due to the distributed propulsion. In fact, this system improves the aerodynamics, allowing better optimum design points, i.e., smaller wings and smaller powertrains. In addition, since the choice of design point influences the aircraft as a whole, the DP system may the a great alternative to obtain more efficient aircraft, which would imply in aircraft that burn less fuel. Thus, for the thin haul aircraft, this technology would fit perfectly to such application, making this kind of operation more profitable and finally present in many small cities.

6. ACKNOWLEDGEMENTS

7. REFERENCES

ACARE, 2012. "Realising europe's vision for aviation: Strategic research innovation agenda, vol. 1".

Bhattacharyya, R.P., Pritchett, A.R. and German, B.J., 2017. "Designing air traffic concepts of operation for thin-haul aviation at small airports". In *2017 IEEE/AIAA 36th Digital Avionics Systems Conference (DASC)*. IEEE, pp. 1–8. DOI: `https://doi.org/10.1109/DASC.2017.8102000`.

Bonet, J.T., Schellenger, H.G., Rawdon, B.K., Elmer, K.R., Wakayama, S.R., Brown, D.L. and Guo, Y., 2011. "Environmentally responsible aviation (era) project-n+ 2 advanced vehicle concepts study and conceptual design of subscale test vehicle (stv) final report".

Borer, N.K., Patterson, M.D., Viken, J.K., Moore, M.D., Bevirt, J., Stoll, A.M. and Gibson, A.R., 2016. "Design and performance of the nasa sceptor distributed electric propulsion flight demonstrator". In *16th AIAA Aviation Technology, Integration, and Operations Conference*. p. 3920. DOI: `https://doi.org/10.2514/6.2016-3920`.

de Vries, R., Brown, M.T. and Vos, R., 2018. "A preliminary sizing method for hybrid-electric aircraft including aeropropulsive interaction effects". In *2018 Aviation Technology, Integration, and Operations Conference*. p. 4228.

Felder, J., Kim, H. and Brown, G., 2009. "Turboelectric distributed propulsion engine cycle analysis for hybrid-wing-body aircraft". In *47th AIAA aerospace sciences meeting including the new horizons forum and aerospace exposition*. p. 1132.

Gohardani, A.S., Doulgeris, G. and Singh, R., 2011. "Challenges of future aircraft propulsion: A review of distributed propulsion technology and its potential application for the all electric commercial aircraft". *Progress in Aerospace Sciences*, Vol. 47, No. 5, pp. 369–391.

Harish, A., Perron, C., Bavaro, D., Ahuja, J., Ozcan, M., Justin, C.Y., Briceno, S.I., German, B.J. and Mavris, D., 2016. "Economics of advanced thin-haul concepts and operations". In *16th AIAA Aviation Technology, Integration, and Operations Conference*. p. 3767.

Hwang, J.T. and Ning, A., 2018. "Large-scale multidisciplinary optimization of an electric aircraft for on-demand mobility". In *2018 AIAA/ASCE/AHS/ASC Structures, Structural Dynamics, and Materials Conference*. p. 1384.

Justin, C.Y., Payan, A.P., Briceno, S.I. and Mavris, D.N., 2017. "Operational and economic feasibility of electric thin haul transportation". In *17th AIAA Aviation Technology, Integration, and Operations Conference*. p. 3283.

NASA, E.R.A., 2012. "N+ 2 advanced vehicle concepts nra draft solicitation synopsis". Technical report, Technical report.

Patterson, M.D., Daskilewicz, M.J. and German, B., 2015. "Simplified aerodynamics models to predict the effects of upstream propellers on wing lift". In *53rd AIAA Aerospace Sciences Meeting*. p. 1673. DOI: `https://doi.org/10.2514/6.2015-1673`.

Raymer, D., 2012. *Aircraft Design: A Conceptual Approach 5e and RDSWin STUDENT*. American Institute of Aeronautics and Astronautics, Inc.

Silva, H.L., 2019. "Contributions to conceptual design of electric and hybrid-electric aircraft".

Stoll, A.M. and Veble Mikic, G., 2016. "Design studies of thin-haul commuter aircraft with distributed electric propulsion". In *16th AIAA Aviation Technology, Integration, and Operations Conference*. p. 3765.

Torenbeek, E., 2013. *Synthesis of subsonic airplane design: an introduction to the preliminary design of subsonic general aviation and transport aircraft, with emphasis on layout, aerodynamic design, propulsion and performance*. Springer Science & Business Media.

8. RESPONSIBILITY NOTICE